SUPPORTING INFORMATION

$Cs_3Zn_6B_9O_{21}$: A Chemically Benign Member of the KBBF Family without Layer Habits Exhibiting the Largest Second Harmonic Generation Response

Hongwei Yu,[†,‡] Hongping Wu,[†] Shilie Pan,[*,†] Zhihua Yang,[†] Xueling Hou,[†] Xin Su,[†] Qun Jing,[†,‡] Kenneth R. Poeppelmeier,[*,§] and James M. Rondinelli[*,δ]

[†] *Key Laboratory of Functional Materials and Devices for Special Environments of CAS; Xinjiang Technical Institute of Physics & Chemistry of CAS, Xinjiang Key Laboratory of Electronic Information Materials and Devices, 40-1 South Beijing Road, Urumqi 830011, China*

[‡] *University of Chinese Academy of Sciences, Beijing 100049, China*

[§]*Department of Chemistry, Northwestern University, 2145 Sheridan Road, Evanston IL 60208-3113, USA*

[δ]*Department of Materials Science and Engineering, Drexel University, Philadelphia, Pennsylvania 19104-2816, United States*

CONTENTS

Synthesis and Single Crystal Growth S2
Structural Refinement and Crystal Data S4
Structure comparison of KBBF and CZB S8
Property Characterization S9
First principles calculations S11
Pseudosymmetry Analysis S15
References S17

1. Experimental Methods

Compound Synthesis. Polycrystalline sample of CZB is prepared by solid-state reaction techniques. All reagents are of analytical grade. A mixture of Cs_2CO_3, ZnO and H_3BO_3 in the molar ratio of 1 : 4 : 6 was ground and loaded into a platinum crucible. The mixture is preheated at 300 °C for 10 h. Then the temperature was raised to 700 °C and held at that temperature for 6 days with several intermediate grindings and mixings.

X-ray powder diffraction analysis of CZB is performed at room temperature in the angular range of 2θ =10° ~70° with a scan step width of 0.02° and a fixed counting time of 1 s/step using a Bruker D2 PHASER diffractometer equipped with a diffracted beam monochromator set for Cu *Kα* radiation (λ = 1.5418 Å). The experimental X-ray powder diffraction pattern did not match any pattern in the database and was later found to be in agreement with the calculated one based the single-crystal crystallographic data of CZB (Figure S1).

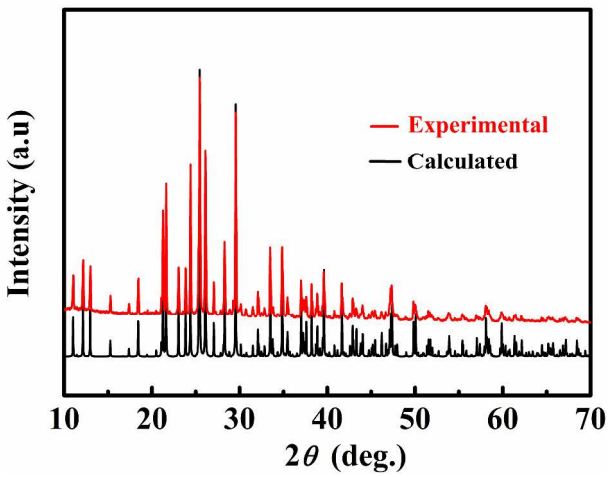

Figure S1. Experimental and calculated X-ray powder diffraction patterns of CZB. The red curve is the experimental pattern, the black one is the calculated one.

Single Crystal Growth. Single crystals of CZB were grown from a high temperature solution using Cs_2O-B_2O_3-PbO as the flux system. The solution was prepared in a platinum crucible by melting a mixture of Cs_2CO_3, ZnO, H_3BO_3 and PbO at a molar ratio of 1 : 1 : 5 : 1. The Pt crucible was placed in the center of a programmable temperature furnace and gradually heated to 750 °C in a programmable temperature until the solution became transparent and clear, and then cools to 650 °C. Then, a platinum wire was promptly dipped into the solution. The temperature was decreased to 550 °C at a rate of 2 °C/h. Then the platinum wire was pulled out of the solution, and allowed to cool to room temperature at a rate of 10 °C/h. Thus a few colorless, transparent crystals were obtained for the structure determination.

Second-order NLO Measurements. The SHG test was performed on the powder sample of CZB by the Kurtz-Perry method.[1] The polycrystalline CZB was ground and sieved into distinct particle size ranges, <20, 20-38, 38-55, 55-88, 88-105, 105-150, and 150-200 μm, and the microcrystalline KDP was also served as a reference. The sample were then placed in a 0.2 mm thick quartz cell and irradiated by a Q-switched Nd:YAG

solid-state laser (1064 nm, 10 kHz, 10 ns). The intensity of the frequency-doubled output emitted from the sample using a photomultiplier tube was measured.

2. Crystal Data and Structural Refinement

Single Crystal X-ray Diffraction. The crystal structure of CZB was determined by single-crystal X-ray diffraction on an APEX II CCD diffractometer using monochromatic Mo *Kα* radiation (λ = 0.71073 Å) at 296(2) K and integrated with the SAINT program.[2] Absorption corrections based on the multiscan technique were also applied. The structure was solved by direct methods using SHELXS-97.[3] All atoms were refined using full matrix least-squares techniques, final least-squares refinement is on F_o^2 with data having $F_o^2 \geq 2\sigma(F_o^2)$. The final difference Fourier synthesis map showed the maximum and minimum peaks at 0.922 and -0.651 e·Å^{-3}, respectively. The structure was checked with PLATON.[4] Crystal data and structure refinement information is given in Table S1. The final refined atomic positions and isotropic thermal parameters are summarized in Table S2. Selected bond lengths and angles for CZB are listed in Table S3.

Table S1. Crystal data and structure refinement for CZB.

Empirical formula	$Cs_3Zn_6B_9O_{21}$
Formula weight	1224.24
Crystal system	Orthorhombic
Space group, Z	$Cmc2_1$, 4
Unit cell dimensions	a = 8.4268(8) Å, b = 19.2101(19) Å, c = 14.5611(14) Å
Volume	2357.1(4) Å^3
Density (calculated)	3.450 Mg/m^3
Absorption coefficient	10.664 /mm
F(000)	2232
Crystal size	0.14 mm × 0.13 mm × 0.04 mm
Theta range for data collection	2.12° to 27.49°
Limiting indices	-10≤ h ≤7, -19≤ k ≤24, -18≤ l ≤18
Reflections collected / unique	7195 / 2873 [R(int) = 0.0245]
Completeness to theta = 27.49	100.0 %
Data / restraints / parameters	2873 / 1 / 191
Goodness-of-fit on F^2	1.006
Final R indices [$F_o^2>2\sigma(F_o^2)$][a]	R1 = 0.0214, wR2 = 0.0445
R indices (all data)[a]	R1 = 0.0245, wR2 = 0.0457
Absolute structure parameter	0.02(2)
Extinction coefficient	0.00009(2)

Table S2. Atomic coordinates (×10^4) and equivalent isotropic displacement parameters (Å^2 × 10^3) and the bond valence sums (BVS) of each atom for CZB. U_{eq} is defined as one-third of the trace of the orthogonalized U_{ij} tensor.

Atom	x	y	z	U(eq)	BVS
Cs(1)	0	1099(1)	2505(1)	27(1)	0.873
Cs(2)	0	1072(1)	-1085(1)	28(1)	0.809
Cs(3)	-5000	28(1)	3221(1)	44(1)	0.836
Zn(1)	3136(1)	1907(1)	771(1)	13(1)	2.141

Zn(2)	1899(1)	2935(1)	2386(1)	13(1)	2.078
Zn(3)	3084(1)	2096(1)	4169(1)	13(1)	2.012
B(1)	0	2760(4)	4072(6)	13(2)	2.99
B(2)	5000	2472(2)	5769(7)	12(1)	3.048
B(3)	2360(5)	332(2)	720(6)	22(1)	3.097
B(4)	2516(10)	4233(4)	1575(5)	24(2)	3.034
B(5)	2436(9)	788(4)	4889(5)	22(2)	3.131
B(6)	5000	2245(4)	2438(7)	11(2)	3.024
O(1)	2250(4)	998(1)	689(5)	30(1)	2.071
O(2)	2388(7)	3906(2)	2370(3)	23(1)	1.975
O(3)	2535(7)	1124(2)	4128(3)	24(1)	2.047
O(4)	-2382(7)	-59(2)	-97(3)	28(1)	2.017
O(5)	2430(4)	1118(1)	5740(4)	33(1)	1.895
O(6)	0	2732(2)	3126(3)	16(1)	2.061
O(7)	1394(3)	2470(1)	1230(2)	14(1)	2.139
O(8)	1423(3)	2766(1)	4525(2)	17(1)	1.998
O(9)	3590(3)	2347(2)	2882(2)	16(1)	1.989
O(10)	5000	2386(2)	4827(3)	14(1)	2.084
O(11)	5000	2044(2)	1535(3)	19(1)	2.051
O(12)	2602(7)	4957(2)	1544(3)	32(1)	2.056

Table S3. Selected bond lengths (Å) and angles (deg) for CZB.

Cs(1)-O(3)	3.187(5)	O(2)#4-Cs(2)-O(4)	83.95(14)
Cs(1)-O(3)#1	3.187(5)	O(2)#5-Cs(2)-O(4)	138.44(10)
Cs(1)-O(1)#1	3.259(6)	O(1)-Cs(2)-O(4)	88.82(12)
Cs(1)-O(1)	3.259(6)	O(1)#1-Cs(2)-O(4)	42.09(10)
Cs(1)-O(6)	3.265(4)	O(10)#5-Cs(2)-O(4)	115.06(10)
Cs(1)-O(12)#2	3.295(5)	O(2)#4-Cs(2)-O(4)#1	138.44(10)
Cs(1)-O(12)#3	3.295(5)	O(2)#5-Cs(2)-O(4)#1	83.95(14)
Cs(1)-O(7)#1	3.430(3)	O(1)-Cs(2)-O(4)#1	42.09(10)
Cs(2)-O(2)#4	3.147(5)	O(1)#1-Cs(2)-O(4)#1	88.82(12)
Cs(2)-O(2)#5	3.147(5)	O(10)#5-Cs(2)-O(4)#1	115.06(10)
Cs(2)-O(1)	3.208(6)	O(4)-Cs(2)-O(4)#1	75.23(19)
Cs(2)-O(1)#1	3.208(6)	O(2)#4-Cs(2)-O(9)#5	85.46(9)
Cs(2)-O(10)#5	3.248(4)	O(2)#5-Cs(2)-O(9)#5	57.19(8)
Cs(2)-O(4)	3.289(5)	O(1)-Cs(2)-O(9)#5	100.31(7)
Cs(2)-O(4)#1	3.289(5)	O(1)#1-Cs(2)-O(9)#5	124.74(7)
Cs(3)-O(2)#6	3.198(5)	O(10)#5-Cs(2)-O(9)#5	53.10(7)
Cs(3)-O(2)#2	3.198(5)	O(4)-Cs(2)-O(9)#5	160.66(10)
Cs(3)-O(3)#1	3.240(5)	O(4)#1-Cs(2)-O(9)#5	122.67(10)
Cs(3)-O(3)#7	3.240(5)	O(2)#4-Cs(2)-O(9)#4	57.19(8)
Cs(3)-O(12)#6	3.284(5)	O(2)#5-Cs(2)-O(9)#4	85.46(9)
Cs(3)-O(12)#2	3.284(5)	O(1)-Cs(2)-O(9)#4	124.74(7)
Cs(3)-O(4)#8	3.296(6)	O(1)#1-Cs(2)-O(9)#4	100.31(7)
Cs(3)-O(4)#9	3.296(6)	O(10)#5-Cs(2)-O(9)#4	53.10(7)
Zn(1)-O(1)	1.902(2)	O(4)-Cs(2)-O(9)#4	122.67(10)

Zn(1)-O(7)	1.943(3)	O(4)#1-Cs(2)-O(9)#4	160.66(10)
Zn(1)-O(11)	1.943(2)	O(9)#5-Cs(2)-O(9)#4	38.63(9)
Zn(1)-O(8)#5	1.955(3)	O(2)#6-Cs(3)-O(2)#2	78.01(18)
Zn(2)-O(2)	1.912(4)	O(2)#6-Cs(3)-O(3)#1	178.09(15)
Zn(2)-O(7)	1.952(3)	O(2)#2-Cs(3)-O(3)#1	101.09(7)
Zn(2)-O(9)	1.956(3)	O(2)#6-Cs(3)-O(3)#7	101.09(7)
Zn(2)-O(6)	1.968(2)	O(2)#2-Cs(3)-O(3)#7	178.09(15)
Zn(3)-O(3)	1.924(4)	O(3)#1-Cs(3)-O(3)#7	79.76(19)
Zn(3)-O(10)	1.959(2)	O(2)#6-Cs(3)-O(12)#6	42.60(11)
Zn(3)-O(8)	1.971(3)	O(2)#2-Cs(3)-O(12)#6	95.99(12)
Zn(3)-O(9)	1.982(3)	O(3)#1-Cs(3)-O(12)#6	139.30(11)
B(1)-O(8)	1.369(5)	O(3)#7-Cs(3)-O(12)#6	84.38(13)
B(1)-O(8)#1	1.369(5)	O(2)#6-Cs(3)-O(12)#2	95.99(12)
B(1)-O(6)	1.378(10)	O(2)#2-Cs(3)-O(12)#2	42.60(11)
B(2)-O(7)#10	1.357(6)	O(3)#1-Cs(3)-O(12)#2	84.38(13)
B(2)-O(7)#11	1.357(6)	O(3)#7-Cs(3)-O(12)#2	139.30(11)
B(2)-O(10)	1.382(11)	O(12)#6-Cs(3)-O(12)#2	83.8(2)
B(3)-O(1)	1.284(4)	O(2)#6-Cs(3)-O(4)#8	136.16(11)
B(3)-O(12)#3	1.400(10)	O(2)#2-Cs(3)-O(4)#8	83.05(13)
B(3)-O(4)#1	1.407(10)	O(3)#1-Cs(3)-O(4)#8	41.93(11)
B(4)-O(2)	1.320(8)	O(3)#7-Cs(3)-O(4)#8	96.55(12)
B(4)-O(5)#5	1.390(9)	O(12)#6-Cs(3)-O(4)#8	178.68(14)
B(4)-O(12)	1.394(8)	O(12)#2-Cs(3)-O(4)#8	96.10(7)
B(5)-O(3)	1.285(8)	O(2)#6-Cs(3)-O(4)#9	83.05(13)
B(5)-O(5)	1.392(9)	O(2)#2-Cs(3)-O(4)#9	136.16(11)
B(5)-O(4)#12	1.401(9)	O(3)#1-Cs(3)-O(4)#9	96.55(12)
B(6)-O(9)#13	1.366(6)	O(3)#7-Cs(3)-O(4)#9	41.93(11)
B(6)-O(9)	1.366(6)	O(12)#6-Cs(3)-O(4)#9	96.10(7)
B(6)-O(11)	1.370(11)	O(12)#2-Cs(3)-O(4)#9	178.68(14)
O(3)-Cs(1)-O(3)#1	84.18(19)	O(4)#8-Cs(3)-O(4)#9	84.00(19)
O(3)-Cs(1)-O(1)#1	173.07(13)	O(1)-Zn(1)-O(7)	103.66(14)
O(3)#1-Cs(1)-O(1)#1	102.28(12)	O(1)-Zn(1)-O(11)	118.55(19)
O(3)-Cs(1)-O(1)	102.28(12)	O(7)-Zn(1)-O(11)	109.75(13)
O(3)#1-Cs(1)-O(1)	173.07(13)	O(1)-Zn(1)-O(8)#5	108.1(2)
O(1)#1-Cs(1)-O(1)	71.16(17)	O(7)-Zn(1)-O(8)#5	106.48(11)
O(3)-Cs(1)-O(6)	77.28(9)	O(11)-Zn(1)-O(8)#5	109.54(13)
O(3)#1-Cs(1)-O(6)	77.28(9)	O(2)-Zn(2)-O(7)	118.85(15)
O(1)#1-Cs(1)-O(6)	106.39(7)	O(2)-Zn(2)-O(9)	114.28(19)
O(1)-Cs(1)-O(6)	106.39(7)	O(7)-Zn(2)-O(9)	102.31(11)
O(3)-Cs(1)-O(12)#2	137.40(11)	O(2)-Zn(2)-O(6)	112.03(19)
O(3)#1-Cs(1)-O(12)#2	85.06(14)	O(7)-Zn(2)-O(6)	101.80(13)
O(1)#1-Cs(1)-O(12)#2	42.19(10)	O(9)-Zn(2)-O(6)	106.03(13)
O(1)-Cs(1)-O(12)#2	88.45(12)	O(3)-Zn(3)-O(10)	119.3(2)
O(6)-Cs(1)-O(12)#2	139.25(10)	O(3)-Zn(3)-O(8)	118.1(2)
O(3)-Cs(1)-O(12)#3	85.06(13)	O(10)-Zn(3)-O(8)	105.71(13)
O(3)#1-Cs(1)-O(12)#3	137.40(11)	O(3)-Zn(3)-O(9)	104.99(16)

O(1)#1-Cs(1)-O(12)#3	88.45(12)	O(10)-Zn(3)-O(9)	102.48(13)
O(1)-Cs(1)-O(12)#3	42.19(10)	O(8)-Zn(3)-O(9)	104.02(12)
O(6)-Cs(1)-O(12)#3	139.25(10)	O(8)-B(1)-O(8)#1	122.3(6)
O(12)#2-Cs(1)-O(12)#3	75.7(2)	O(8)-B(1)-O(6)	118.8(3)
O(3)-Cs(1)-O(7)#1	128.28(8)	O(8)#1-B(1)-O(6)	118.8(3)
O(3)#1-Cs(1)-O(7)#1	99.23(9)	O(7)#10-B(2)-O(7)#11	119.9(8)
O(1)#1-Cs(1)-O(7)#1	53.67(6)	O(7)#10-B(2)-O(10)	120.0(4)
O(1)-Cs(1)-O(7)#1	78.82(8)	O(7)#11-B(2)-O(10)	120.0(4)
O(6)-Cs(1)-O(7)#1	54.00(7)	O(1)-B(3)-O(12)#3	122.9(8)
O(12)#2-Cs(1)-O(7)#1	94.11(10)	O(1)-B(3)-O(4)#1	120.3(8)
O(12)#3-Cs(1)-O(7)#1	119.46(10)	O(12)#3-B(3)-O(4)#1	116.8(3)
O(2)#4-Cs(2)-O(2)#5	88.75(18)	O(2)-B(4)-O(5)#5	122.7(5)
O(2)#4-Cs(2)-O(1)	171.71(12)	O(2)-B(4)-O(12)	120.4(6)
O(2)#5-Cs(2)-O(1)	99.38(13)	O(5)#5-B(4)-O(12)	116.9(6)
O(2)#4-Cs(2)-O(1)#1	99.38(13)	O(3)-B(5)-O(5)	122.6(6)
O(2)#5-Cs(2)-O(1)#1	171.71(12)	O(3)-B(5)-O(4)#12	121.1(6)
O(1)-Cs(2)-O(1)#1	72.46(17)	O(5)-B(5)-O(4)#12	116.2(6)
O(2)#4-Cs(2)-O(10)#5	106.27(8)	O(9)#13-B(6)-O(9)	120.8(8)
O(2)#5-Cs(2)-O(10)#5	106.27(8)	O(9)#13-B(6)-O(11)	119.6(4)
O(1)-Cs(2)-O(10)#5	73.18(7)	O(9)-B(6)-O(11)	119.6(4)
O(1)#1-Cs(2)-O(10)#5	73.18(7)		

Symmetry transformations used to generate equivalent atoms:
#1 -x,y,z #2 x-1/2,y-1/2,z #3 -x+1/2,y-1/2,z
#4 x-1/2,-y+1/2,z-1/2 #5 -x+1/2,-y+1/2,z-1/2
#6 -x-1/2,y-1/2,z #7 x-1,y,z #8 x,-y,z+1/2
#9 -x-1,-y,z+1/2 #10 x+1/2,-y+1/2,z+1/2
#11 -x+1/2,-y+1/2,z+1/2 #12 -x,-y,z+1/2
#13 -x+1,y,z #14 x+1/2,y+1/2,z #15 x+1,y,z
#16 -x,-y,z-1/2 #17 -x-1,-y,z-1/2
#18 -x+1/2,y+1/2,z

3. The comparison of KBBF and CZB

In KBBF, within the *ab* plane strong covalent bonding of B – O – Be exists, whereas along *c* direction only weak ionic bonding of largely separated K^+ and F^- ions is present. In the structure of CZB, it is worth noted that the adjacent $[Zn_2BO_3O_2]_\infty$ layers are connected by the B_3O_6 planar groups, the interlayer connection of $[Zn_2BO_3O_2]_\infty$ layers afforded by the strong covalent bonding of B_3O_6 groups more stronger than that of the K^+–F^- ionic bonds, which suggests CZB will grow without layer habits. These also can be observed the growth crystal (Figure S2).

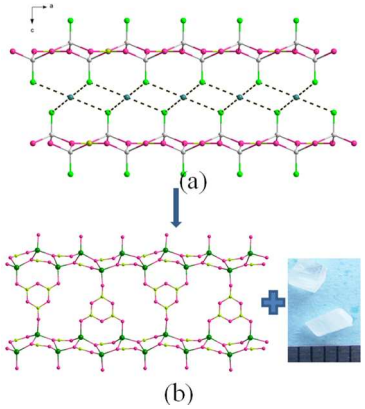

Figure S2.(a) View along the *b* axis for the structure of KBBF. (b) View along the *a* axis for the structure of CZB, and the photograph of CZB crystals.

4. Optical Characterization

Infrared Spectroscopy. Infrared spectrum in the 400-4000 cm^{-1} range was recorded on Shimadzu IR Affinity-1 Fourier transform infrared spectrometer in order to specify and compare the coordination of boron in CZB. The sample was mixed thoroughly with dried KBr and the characteristic absorption peaks were shown in Figure S3.

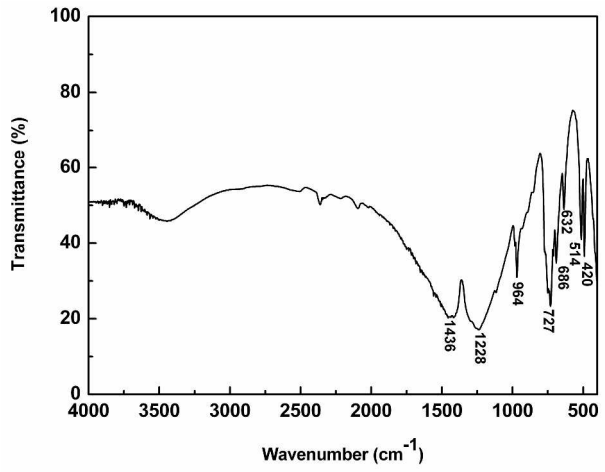

Figure S3. IR spectrum of CZB.

UV-vis-NIR Diffuse Reflectance Spectrum. Optical diffuse reflectance spectrum was measured at room temperature with Shimadzu SolidSpec-3700DUV spectrophotometer. Data were collected in the wavelength range 190–2600 nm.

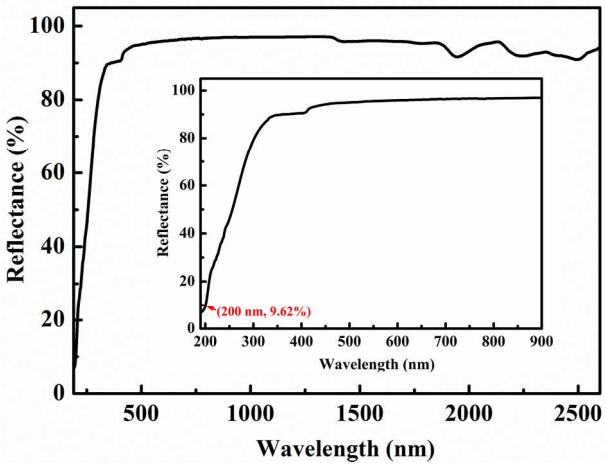

Figure S4. The diffuse reflectance spectrum of CZB.

Thermal Analysis. The thermal analysis was carried out on a simultaneous NETZSCH STA 449C simultaneous analyzer under N_2. The sample and reference (Al_2O_3) were enclosed in Pt crucibles, heated from room temperature to 1200 °C at a rate of 10 °C/min.

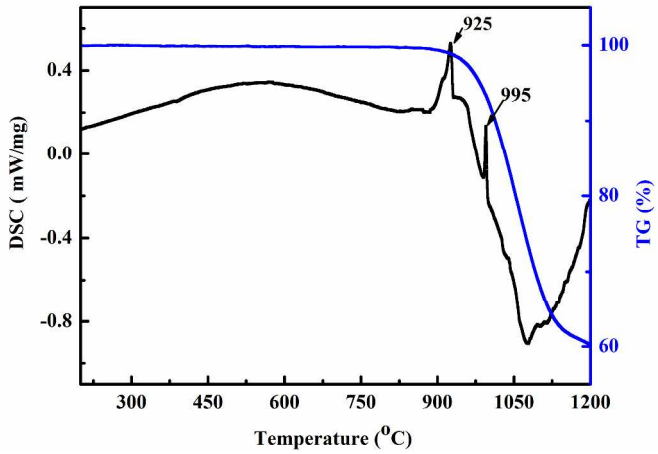

Figure S5. TG/DSC curves of CZB.

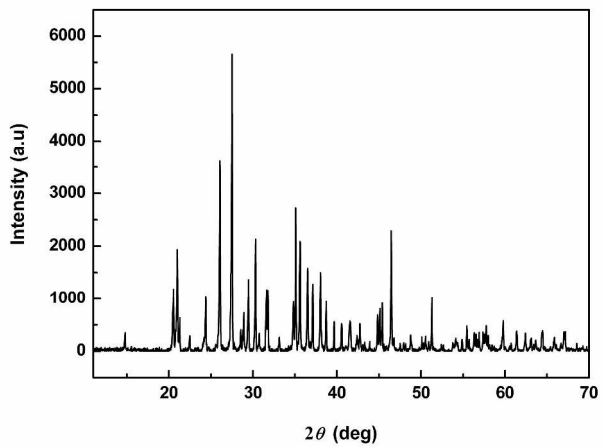

Figure S6. X-ray powder diffraction pattern of the residue in the platinum pan after TG/DSC measurement.

4. **First principles calculations.**

The electronic structure of CZB was computed using density functional theory (DFT) based as implemented in the plane-wave CASTEP package,[6] with the local density approximation (LDA) using the Perdew-Zunger parameterization of the Ceperley-Alder (CA-PZ) data[7,8] for the exchange and correlation functional. A plane-wave energy cutoff of 750 eV was used and norm-conserving pseudopotentials to treat the interaction between the core and valence electrons. The Monkhorst-Pack scheme[5] and a 4 × 4 × 2 *k*-point mesh was used in the calculations to sample the Brillouin zone.

The SHG coefficients are calculated via the reduced length-gauge formalism developed by J. Lin[9] from the formalism proposed by Aversa and Sipe[10, 11] at the zero-frequency limit. The static second-order nonlinear susceptibilities $\chi_{\alpha\beta\gamma}^{(2)}$ can be reduced as:

$$\chi_{\alpha\beta\gamma}^{(2)} = \chi_{\alpha\beta\gamma}^{(2)}(\mathrm{VE}) + \chi_{\alpha\beta\gamma}^{(2)}(\mathrm{VH}) + \chi_{\alpha\beta\gamma}^{(2)}(\text{two-bands}) \quad (1)$$

$$\chi_{\alpha\beta\gamma}^{(2)}(VE) = \frac{e^3}{2\hbar m^3}\sum_{vv'c}\int\frac{d^3k}{4\pi^3}P(\alpha\beta\gamma)\,\mathrm{Im}\left[P_{vv'}^{\alpha}P_{cv'}^{\beta}P_{cv}^{\gamma}\right]\left(\frac{1}{\omega_{cv}^3\omega_{v'c}^2}+\frac{2}{\omega_{vc}^4\omega_{cv'}}\right) \quad (2)$$

$$\chi_{\alpha\beta\gamma}^{(2)}(VH) = \frac{e^3}{2\hbar m^3}\sum_{vcc'}\int\frac{d^3k}{4\pi^3}P(\alpha\beta\gamma)\,\mathrm{Im}\left[P_{cv}^{\alpha}P_{cc'}^{\beta}P_{c'v}^{\gamma}\right]\left(\frac{1}{\omega_{cv}^3\omega_{vc'}^2}+\frac{2}{\omega_{vc}^4\omega_{c'v}}\right) \quad (3)$$

$$\chi_{\alpha\beta\gamma}^{(2)}(two-bands) = \frac{e^3}{2\hbar m^3}\sum_{vc}\int\frac{d^3k}{4\pi^3}P(\alpha\beta\gamma)\frac{\mathrm{Im}\left[P_{vc}^{\alpha}P_{cv}^{\beta}(P_{vv}^{\gamma}-P_{cc}^{\gamma})\right]}{\omega_{vc}^5} \quad (4)$$

where $\chi_{\alpha\beta\gamma}^{(2)}$ (VE), $\chi_{\alpha\beta\gamma}^{(2)}$ (VH), $\chi_{\alpha\beta\gamma}^{(2)}$ (two-bands) denote the contributions from virtual-electron (VE), virtual-hole (VH), and two-band processes to $\chi_{\alpha\beta\gamma}^{(2)}$, respectively. The α, β and γ subscripts are Cartesian components of the tensor, v and v′ denote valence bands, c and c′ denote conduction bands, and P (αβγ) denotes full permutation. The band energy difference and momentum matrix elements are denoted as $\hbar\omega_{ij}$ and P_{ij}^{α}, respectively.

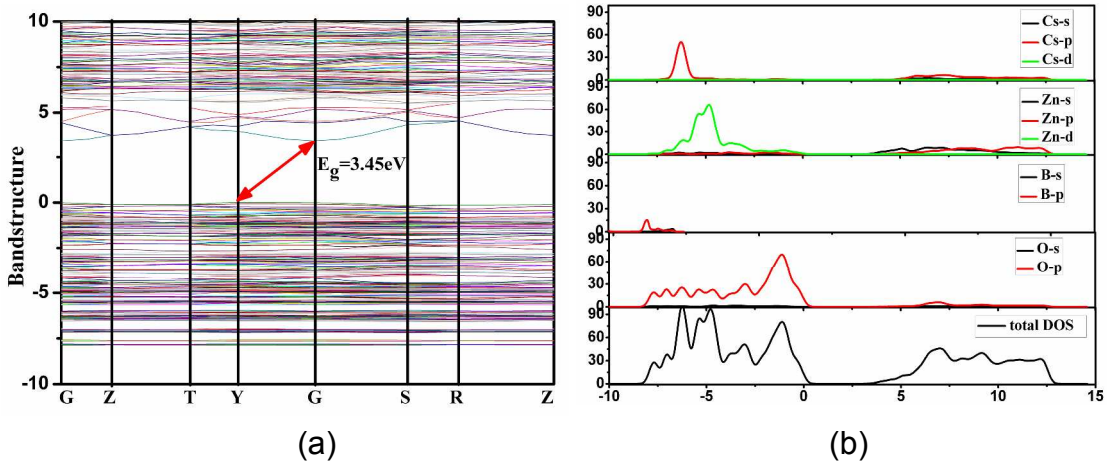

Figure S7. Calculated band structure (a) and densities of states of CZB (b).

The calculation of electronic band structures shows that CZB is an indirect gap compound and the LDA band gap is 3.45 eV. In order to compare the calculated optical gap and experimental one, the UV-Vis-NIR diffuse reflectance spectrum (Figure S4) was converted to absorbance with the Kubelka-Munk function.[12,13] And since CZB is an indirect band compound, the band gap should be obtained from the plots of $(h\nu F(R))^{1/2}$ versus $h\nu$.[14,15] On the plots of $(h\nu F(R))^{1/2}$ versus $h\nu$, extrapolating the linear part of the rising curve to zero shows that the band gap of CZB is 4.13 eV, which is consistent with the calculated value.

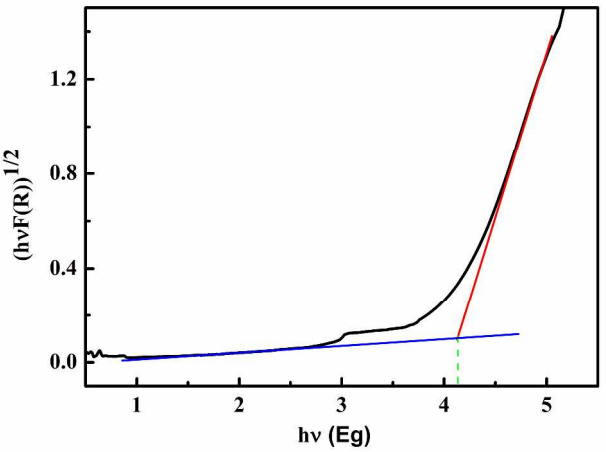

Figure S8. Optical absorption spectrum of CZB.

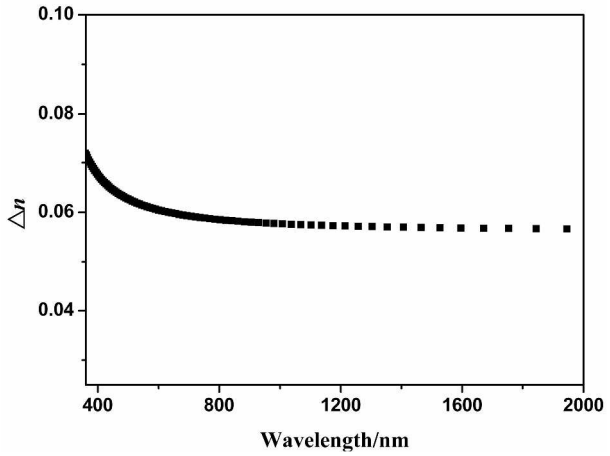

Figure S9. The curve of birefringence (Δ*n*) versus wavelength.

5. Pseudosymmetry Analysis.

Table S4. Crystallographic data for the pseudosymmetric *Cmcm* structure of CZB with *a*=8.42680 Å, *b*=19.2101 Å, and *c*=14.5611 Å.

Atom	**Wyckoff Site**	***x***	***y***	***z***
Cs(1)	8*f*	0	0.3915	0.0705
Cs(3)	4*a*	0	0	0.5
Zn(1)	8*g*	0.3136	0.3093	0.25
Zn(2)	16*h*	0.1908	0.2081	0.08915
B(1)	8*f*	0	0.7758	0.4183
B(2)	4*c*	0	0.2472	0.25
B(3)	8*g*	0.2360	0.4668	0.25
B(4)	16*h*	0.2540	0.0778	0.1657
O(1)	8*g*	0.2250	0.4002	0.25
O(2)	16*h*	0.2427	0.1109	0.0879
O(5)	8*g*	0.2570	0.1118	0.25
O(7)	8*g*	0.1394	0.2530	0.25
O(8)	16*h*	0.3584	0.2710	0.4179
O(10)	8*f*	0	0.2327	0.4150
O(11)	4*c*	0	0.2044	0.75
O(12)	16*h*	0.2610	0.0051	0.1680

A similar analysis is performed for KBBF which exhibits a chiral ground state structure *R*32 (space group 155) using the experimental data from ICSD (entry 155156, *J. Cryst. Growth* **2006**, *293*, 233).

The pseudosymmetric reference phase for KBBF has $R\bar{3}m$ symmetry (space group 166) with *a*=4.4261 Å, *b*=4.4261 Å, and *c*=18.7617 Å. The crystallographic data is given in Table S5.

Atom	**Wyckoff Site**	***x***	***y***	***z***
K	3*b*	0	0	0.5
F	6*c*	0	0	0.2217
O	9*e*	0.5	0	0
B	3*a*	0	0	0
Be	6*c*	0	0	0.3024

These two phases are related by a single irrep (Γ_1^-) and involves only displacements of the oxygen atoms in the *ab*-plane in a "screw" fashion about the Be atoms—this gives rise to the handiness in the structure. Figure S10a shows the displacement pattern plotted in an unconventional way to highlight the O-O network to emphasize this aspect.

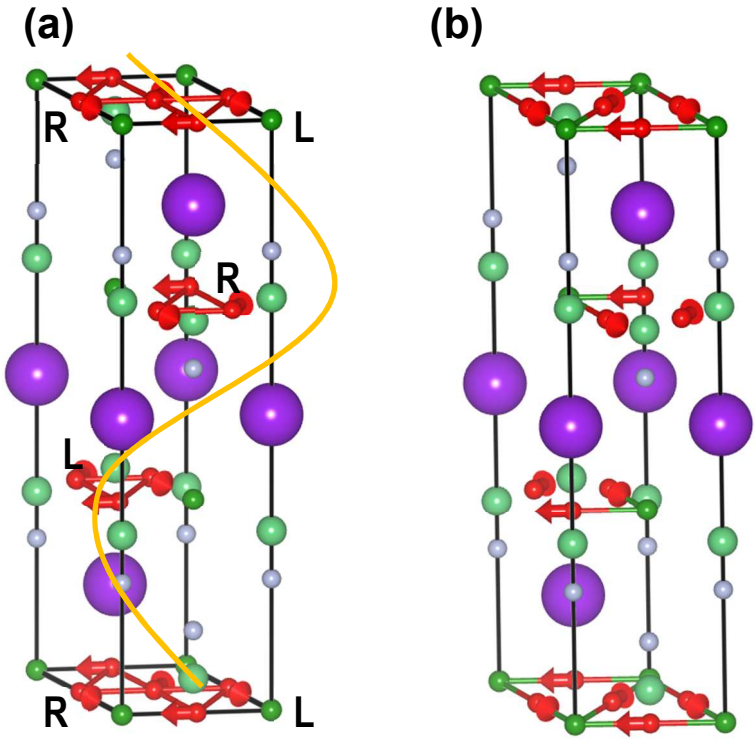

Figure S10. The Γ_1^- displacement pattern in KBBF with (a) O-O rings highlighted and (b) BO_3 rings emphasized. Key: Red (oxygen), green atoms on corners (boron), light green (beryllium), purple (potassium)

Examining the displacement pattern now with respect to the BO_3 units (Figure S10b), makes it clear that the triangular BO_3 units are all uniform (regular). Unlike CZB there are no polar displacements in KBBF, which is not surprising as the distorted KBBF structure is only chiral.

References

(1) Kurtz, S. K.; Perry, T. T. *J. Appl. Phys.* **1968**, *39*, 3798.

(2) SAINT, version 7.60A; Bruker Analytical X-ray Instruments, Inc.: Madison, WI, **2008**.

(3) Sheldrick, G. M. SHELXTL, version 6.14; Bruker Analytical X-ray Instruments, Inc.: Madison, WI, **2003**.

(4) Spek, A. L. *J. Appl. Crystallogr.* **2003**, *36*, 7., G.; Joubert, D. *Phys. Rev. B* **1999**, *59*, 1758.

(5) Clark, S. J.; Segall, M. D.; Pickard, C. J.; Hasnip, P. J.; Probert, M. J.; Refson, K.; Payne, M. C. *Z. Kristallogr.* **2005,** *220*, 567.

(6) Ceperley, D. M.; Alder, B. J. *Phys. Rev. Lett.* **1980,** *45*, 566.

(7) Perdew, J. P.; Zunger, A. *Phys. Rev. B.* **1981**, *23*, 5048.

(8) Monkhorst, H. J.; Pack, J. D. *Phys. Rev. B.* **1976**, *13*, 5188.

(9) Lin, J.; Lee, M. H.; Liu, Z.P.; Chen, C.T.; Pickard, C. J. *Phys. Rev. B* **1999**, *60*, 51.

(10) Rashkeev, S. N.; Lambrecht, W. R. L.; Segall, B. *Phys. Rev. B* **1998**, *57*, 3905.

(11) Aversa, C.; Sipe, J. E. *Phys. Rev. B* **1995**, *52*, 14636.

(12) Kubelka, P.; Munk, F. Z.; *Tech. Phys.*, **1931**, *12*, 593.

(13) Tauc, J.; *Mater. Res. Bull.*, **1970,** *5*, 721.

(14) Bang, T. H.; Choe, S. H.; Park, B. N.; Jin, M. S.; Kim, W. T. *Semicond. Sci. Technol.* **1996**, *11*, 1159.

(15) Mitchell, K.; Huang, F. Q.; McFarland, A. D.; Haynes, C. L.; Somers, R. C.; Van Duyne, R. P.; Ibers, J. A. *Inorg. Chem.* **2003**, *42*, 4109.